

FOURIER PHASE RETRIEVAL WITH A SINGLE MASK BY DOUGLAS-RACHFORD ALGORITHM

PENGWEN CHEN AND ALBERT FANNJIANG

ABSTRACT. Douglas-Rachford (DR) algorithm is analyzed for Fourier phase retrieval with a single random phase mask. Local, geometric convergence to a unique fixed point is proved with numerical demonstration of global convergence.

KEYWORDS. Phase retrieval, diffract-before-destruct, coded diffraction pattern, Douglas-Rachford algorithm

1. INTRODUCTION

X-ray crystallography has been the preferred technology for determining the structure of a biological molecule over the past hundred years. The method, however, is limited by crystal quality, radiation damage and phase determination [46]. The first two problems call for large crystals that yield sufficient diffraction intensities while reducing the dose to individual molecules in the crystal. The difficulty of growing large, well-diffracting crystals is thus the major bottleneck of X-ray crystallography - a necessary experimental step that can range from merely challenging to pretty much impossible, particularly for large macromolecular assemblies and membrane proteins.

By boosting the brightness of available X-rays by 10 orders of magnitude and producing pulses well below 100 fs duration, X-ray free electron lasers (XFEL) offer the possibility of extending structural studies to *single, non-crystalline* particles or molecules by using short intense pulses that out-run radiation damage, thus circumventing the first two aforementioned problems [48]. In the so-called *diffract-before-destruct* approach [19, 20, 53], a stream of particles is flowed across the XFEL beam and randomly hit by a single X-ray pulse, forming a single diffraction pattern before being vaporized as a nano-plasma burst. Each diffraction pattern contains certain information about the planar projection of the scattering potential of the object along the direction of the beam which is to be recovered by phase retrieval techniques [10].

The modern approach to phase retrieval for non-periodic objects roughly starts with the Gerchberg-Saxton algorithm [32], followed by its variant, Error Reduction (ER), and the more powerful Hybrid-Input-Output (HIO) algorithm [30, 31]. These form the cornerstones of the standard *iterative transform algorithms* (ITA) [8, 41].

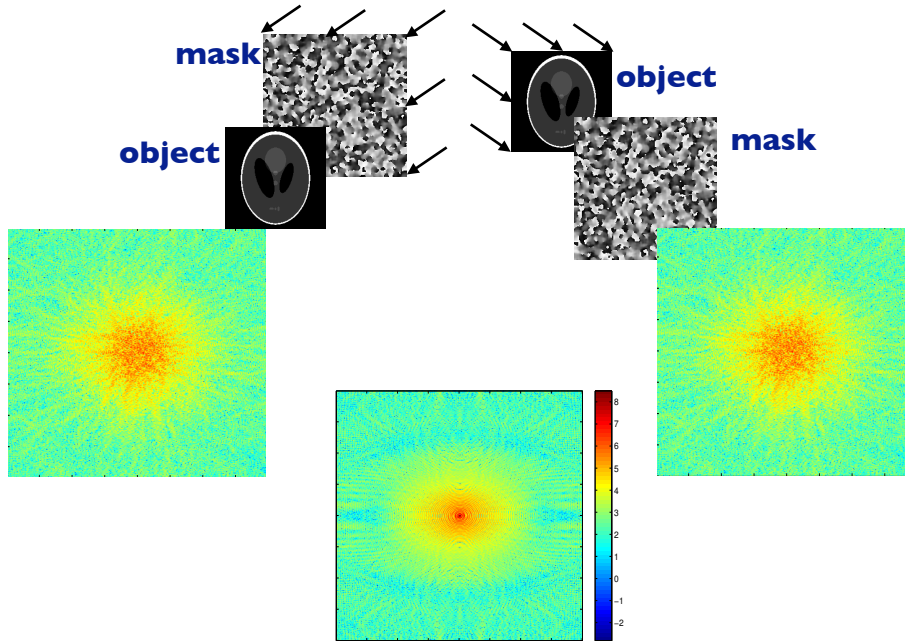


FIGURE 1. Conceptual layout of coherent lensless imaging with a random mask (left) *before* (for random illumination) or (right) *behind* (for wavefront sensing) the object. (middle) The diffraction pattern measured without a mask has a larger dynamic range. The color bar is on a logarithmic scale.

However, the standard ITA tend to stagnate and do not perform well without additional prior information, such as tight support and positivity. The reason is that the *plain* diffraction pattern alone does not guarantee uniqueness of solution (see [52], however, for uniqueness under additional prior information). On the contrary, many phasing solutions exist for a given diffraction pattern, resulting in what is called the *phase* problem [35].

To this end, a promising approach is to measure the diffraction pattern with a *single* random mask and use the coded diffraction pattern as the data. As shown in [27], the uniqueness of solution is restored with a high probability given any scattering potential whose value is restricted to a known sector (say, the upper half plane) of the complex plane (see Proposition 6.1).

Indeed, the sector constraint is a practical, realistic condition to impose on almost all materials as the imaginary part of the scattering potential is proportional to the (positive) extinction coefficient with the upper half plane as the sector constraint [10]. For X-ray regime, the real part of the scattering potential is typically slightly negative which with a nonnegative imaginary part gives to the second quadrant as the sector constraint [17].

What happens if the sector condition is not met and consequently one coded diffraction pattern is not enough to ensure uniqueness? This question is particularly pertinent to the diffract-before-destroy approach as the particle can not withstand the radiation damage from more than one XFEL pulses.

A plausible measurement scheme is to guide the transmitted field (the transmission function [10]) from a *planar* illumination through a beam splitter [50], generating two copies

of the transmitted field which are then measured separately as a coded diffraction pattern and a plain diffraction pattern. In this set-up, the object function is the transmitted field behind the particle and the phase retrieval problem becomes the wave-front reconstruction problem [10, 34]. In practice beam splitters and the masks (or any measurement devices) should be used as sparingly as possible to avoid introducing excessive measurement noises.

With two diffraction patterns, the uniqueness of solution (in the above sense) is restored almost surely without the sector constraint (see Proposition 6.1 and Remark 6.3).

With the uniqueness-ensuring sampling schemes (Section 1.1), *ad hoc* combinations of members of ITA (such as HIO and ER) can be devised to recover the true solution [28, 29]. There is, however, no convergence proof for these algorithms.

The main goal of the paper is to prove the *local, geometric convergence* of the Douglas-Rachford (DR) algorithm to a unique fixed point in the case of one or two oversampled diffraction patterns (Theorems 4.1, 5.3 and 6.2) and demonstrate *global convergence* numerically (Section 7).

DR has the following general form: Let P_1 and P_2 be the projections onto the two constraint sets, respectively. For phase retrieval, P_1 describes the projection onto the set of diffracted fields (instead of diffraction patterns) and P_2 the data fitting. The Douglas-Rachford (DR) algorithm is defined by the iteration scheme [24, 39]

$$(1) \quad y^{(k+1)} = y^{(k)} + P_1(2P_2 - I)y^{(k)} - P_2y^{(k)}, \quad k = 1, 2, 3, \dots$$

Closely related to HIO, DR also belongs to the ITA family (Section 3). ITA are computationally efficient thanks to the fast Fourier transform (FFT) and explicit nature of P_1, P_2 (see (11) below).

1.1. Oversampled diffraction patterns. Next we describe our sampling schemes before we can properly introduce P_1, P_2 and the Douglas-Rachford algorithm for phase retrieval (Section 3).

Let $f(\mathbf{n})$ be a discrete object function with $\mathbf{n} = (n_1, n_2, \dots, n_d) \in \mathbb{Z}^d$. Consider the object space consisting of all functions supported in $\mathcal{M} = \{0 \leq m_1 \leq M_1, 0 \leq m_2 \leq M_2, \dots, 0 \leq m_d \leq M_d\}$. We assume $d \geq 2$.

With a coherent illumination under the Fraunhofer approximation, the free-space propagation between the object plane and the sensor plane can be described by the Fourier transform [10] (with the proper coordinates and normalization). However, only the *intensities* of the Fourier transform are measured on the sensor plane and constitute the so called *diffraction pattern* given by

$$\sum_{\mathbf{n}=-\mathbf{M}}^{\mathbf{M}} \sum_{\mathbf{m}+\mathbf{n} \in \mathcal{M}} f(\mathbf{m} + \mathbf{n}) \overline{f(\mathbf{m})} e^{-i2\pi \mathbf{n} \cdot \mathbf{w}}, \quad \mathbf{w} = (w_1, \dots, w_d) \in [0, 1]^d, \quad \mathbf{M} = (M_1, \dots, M_d)$$

which is the Fourier transform of the autocorrelation

$$R_f(\mathbf{n}) = \sum_{\mathbf{m} \in \mathcal{M}} f(\mathbf{m} + \mathbf{n}) \overline{f(\mathbf{m})}.$$

Here and below the over-line notation means complex conjugacy.

Note that R_f is defined on the enlarged grid

$$\widetilde{\mathcal{M}} = \{(m_1, \dots, m_d) \in \mathbb{Z}^d : -M_1 \leq m_1 \leq M_1, \dots, -M_d \leq m_d \leq M_d\}$$

whose cardinality is roughly 2^d times that of \mathcal{M} . Hence by sampling the diffraction pattern on the grid

$$\mathcal{L} = \left\{ (w_1, \dots, w_d) \mid w_j = 0, \frac{1}{2M_j + 1}, \frac{2}{2M_j + 1}, \dots, \frac{2M_j}{2M_j + 1} \right\}$$

we can recover the autocorrelation function by the inverse Fourier transform. This is the *standard oversampling* with which the diffraction pattern and the autocorrelation function become equivalent via the Fourier transform [43, 44].

A coded diffraction pattern is measured with a mask whose effect is multiplicative and results in a *masked object* of the form $g(\mathbf{n}) = f(\mathbf{n})\mu(\mathbf{n})$ where $\{\mu(\mathbf{n})\}$ is an array of random variables representing the mask. In other words, a coded diffraction pattern is just the plain diffraction pattern of a masked object.

We will focus on the effect of *random phases* $\phi(\mathbf{n})$ in the mask function $\mu(\mathbf{n}) = |\mu|(\mathbf{n})e^{i\phi(\mathbf{n})}$ where $\phi(\mathbf{n})$ are independent, continuous real-valued random variables and $|\mu|(\mathbf{n}) \neq 0, \forall \mathbf{n} \in \mathcal{M}$ (i.e. the mask is transparent).

Without loss of generality, we assume $|\mu(\mathbf{n})| = 1, \forall \mathbf{n}$ which gives rise to a *phase* mask and an *isometric* propagation matrix

$$(2) \quad (1\text{-mask}) \quad A^* = c\Phi \text{diag}\{\mu\},$$

i.e. $AA^* = I$ (with a proper choice of the normalizing constant c), where Φ is the *oversampled* d -dimensional discrete Fourier transform (DFT). Specifically $\Phi \in \mathbb{C}^{|\tilde{\mathcal{M}}|, |\mathcal{M}|}$ is the sub-column matrix of the standard DFT on the extended grid $\tilde{\mathcal{M}}$ where $|\mathcal{M}|$ is the cardinality of \mathcal{M} .

When two phase masks μ_1, μ_2 are deployed, the propagation matrix A^* is the stacked coded DFTs, i.e.

$$(3) \quad (2\text{-mask case}) \quad A^* = c \begin{bmatrix} \Phi \text{diag}\{\mu_1\} \\ \Phi \text{diag}\{\mu_2\} \end{bmatrix}$$

With proper normalization, A^* is isometric.

In line with the spirit of simplifying measurement complexity discussed above, we remove the second mask (i.e. $\mu_2 \equiv 1$) and consider the propagation matrix [27–29]

$$(4) \quad (1\frac{1}{2}\text{-mask case}) \quad A^* = c \begin{bmatrix} \Phi \text{diag}\{\mu\} \\ \Phi \end{bmatrix}$$

normalized to be isometric, where μ is independently and continuously distributed over the unit circle. In other words, one oversampled coded pattern and one oversampled plain pattern are used for reconstruction.

For convenience, we shall refer to this set-up as the $1\frac{1}{2}$ -mask case to distinguish it from the one- and two-mask cases. This and its extension to the multi-mask cases would be the set-up for all our numerical simulations in Section 7.

1.2. Related literature. For the optical spectrum, experiments with coded diffraction patterns are not new and can be implemented by computer generated holograms [11], random phase plates [1] and liquid crystal phase-only panels [26]. Recently, a phase mask with randomly distributed pinholes has been implemented for soft X-ray [40].

Coded-aperture phase retrieval was formulated as a convex trace-norm minimization problem in [12, 15, 18] whose uniqueness was proved in [14] under the assumption that the number of independently coded diffraction patterns is sufficiently large (polylogarithmic in $|\mathcal{M}|$).

The convex formulation [12, 14, 15] certainly has a tremendous appeal as global convergence can be expected for any proper numerical implementations. However, due to the lift to much higher dimensions, the convex program may be computationally expensive (see also [7, 33]).

Alternative non-convex minimization formulations were proposed and solved by various gradient methods [13, 45]. In practice, these algorithms are locally convergent with a comparatively large number (≥ 6) of coded diffraction patterns.

An important difference between the measurement schemes in these papers and the present work (as well as [27–29]) is that their coded diffraction patterns are *not* oversampled. Another distinctive feature of the present setting is that the dimension $d \geq 2$ is required for the spectral gap (Theorem 5.3) and the uniqueness of fixed point (Theorem 6.2), but not for the structure theorem (Theorem 4.1).

In this connection, we emphasize that reducing the number of coded diffraction patterns is crucial for the diffract-before-destruct approach and, in our view, oversampling is a small price to pay with current sensor technologies.

A bigger price may be that we lose the robust injectivity property prized in these works (also see [5, 6]). In other words, just one or two random masks, the phase retrieval map F defined as $F(x) \equiv |A^*x|$ with A^* given by (4) or (3) is injective only after a certain finite set is excluded from \mathbb{C}^M . On the other hand, for any given f , with probability one the selection of the mask(s) is such that no other object, modulo a phase factor, produces the same data as $|A^*f|$ with A^* given by (4) or (3). Our numerical results show that this notion of uniqueness appears suffices for most practical purposes when DR is implemented for phase retrieval.

However, to the best of our knowledge, even local convergence is not known for any ITA for Fourier phase retrieval. The present paper aims to fill this gap. While we can not prove *global* convergence of DR as for the convex setting, we will present strong numerical evidence for global convergence. In [21], we prove the local, geometric convergence of the error reduction algorithm with the same measurement scheme described in Section 1.1. Local convergence of ER in the case of Gaussian matrix A^* was recently proved in [47].

There is much more literature on phase retrieval with generic frames and independent random matrices [2–6, 15, 16, 22, 25, 54, 56] which have a somewhat different flavor from that with Fourier phase retrieval as the latter is neither of the former two. Consequently, some of our results (Theorems 5.3 and 6.2) can not extend to these other cases without major revision. The structure theorem (Theorem 4.1) remains valid, however (see Remark 4.4).

There also is a growing body of work on phase retrieval under sparsity assumptions, see [37, 38, 49, 51] and the references therein.

The rest of the paper is organized as follows. In Section 2, we simplify the notation for presenting the main results and the proof of local convergence. In Section 3, we describe the DR algorithm widely used in convex optimization problems and formulate it for the non-convex problem of phase retrieval. In Section 4, we prove local convergence of FDR under the spectral gap assumption (Theorem 4.1). In Section 5, we prove the spectral gap condition for any number of oversampled diffraction patterns (Theorem 5.3). In Section 6, we prove that the fixed point of DR is unique for one or two oversampled diffraction patterns (Theorem 6.2). In Section 7 we give numerical examples and demonstrate global convergence of the DR scheme.

2. SET-UP AND NOTATION

For the main text below, we shall simplify the notion as follows. The more elaborate notion of Section 1.1 will be useful again in the appendix.

First, we convert the d -dimensional grid into an ordered set of index. The unknown object will now be denoted by $x_0 \in \mathbb{C}^n, n = |\mathcal{M}|$. In other words, x_0 is the vectorized version of the object function f supported in $\mathcal{M} \subset \mathbb{Z}^d, d \geq 2$ (Section 1.1).

Rank-2 property: x_0 is rank-2 (or higher) if the convex hull of $\text{supp}\{f\}$ is two (or higher) dimensional.

Let \mathcal{X} be a nonempty closed convex set in \mathbb{C}^n and

$$(5) \quad [x]_{\mathcal{X}} = \arg \min_{x' \in \mathcal{X}} \|x' - x\|$$

the projection onto \mathcal{X} .

Sector constraint: x_0 satisfies the sector constraint if the principal value of $\arg x_0(j), \forall j$ is restricted to a *sector* $[-\alpha\pi, \beta\pi] \subsetneq (-\pi, \pi], \forall \mathbf{n}$. As mentioned above almost all scattering potentials f have a nonnegative imaginary part and hence satisfy the sector constraint with $\alpha = 0, \beta = 1$. The sector constraint serves as transition between the standard positivity constraint ($\alpha = \beta = 0$) and the null constraint ($\alpha = \beta = 1$).

The sector projection is explicitly given as follows: For $j \leq n$

$$(6) \quad [x]_{\mathcal{X}}(j) = \begin{cases} x(j) & \text{if } \angle x(j) \in [-\alpha\pi, \beta\pi] \\ \Re[x(j)e^{-i\beta\pi}]e^{i\beta\pi} & \text{if } \angle x(j) \in [\beta\pi, (\beta + 1/2)\pi] \\ \Re[x(j)e^{i\alpha\pi}]e^{-i\alpha\pi} & \text{if } \angle x(j) \in [-(\alpha + 1/2)\pi, -\alpha\pi] \\ 0 & \text{else} \end{cases}$$

and $[x]_{\mathcal{X}}(j) = 0, j > n + 1$.

Phase retrieval problem. For a given unknown object x_0 of rank ≥ 2 , let $A^* = [a_j^*] \in \mathbb{C}^{N \times n}$ be the propagation matrix given by (2), (3) or (4) where A^* is normalized to be isometric and $b = |A^*x_0| \in \mathbb{R}^N$ be the data vector. Phase retrieval is to find a solution x to the equation

$$(7) \quad b = |A^*x|, \quad x \in \mathcal{X}.$$

We focus on two cases.

1) One-pattern case: A^* is given by (2), $[x]_{\mathcal{X}}$ is given by (6).

2) Two-pattern case: A^* is given by (3) or (4), $\mathcal{X} = \mathbb{C}^n$.

Phasing solution is unique only up to a constant of modulus one no matter how many coded diffraction patterns are measured. Thus the proper error metric for an estimate \hat{x} of the true solution x_0 is given by

$$(8) \quad \min_{\theta \in \mathbb{R}} \|e^{-i\theta}x_0 - \hat{x}\| = \min_{\theta \in \mathbb{R}} \|e^{i\theta}\hat{x} - x_0\|.$$

Throughout the paper, we assume the canonical embedding

$$\mathbb{C}^n \subseteq \mathbb{C}^{\tilde{n}} \subseteq \mathbb{C}^N, \quad n \leq \tilde{n} \leq N.$$

For example, if $x \in \mathbb{C}^n$, then the embedded vector in $\mathbb{C}^{\tilde{n}}$ or \mathbb{C}^N , still denoted by x , has zero components $x(j) = 0$ for $j \geq n+1$. This is referred to as *zero padding* and \tilde{n}/n is the *padding ratio*. Conversely, if $x \in \mathbb{C}^{\tilde{n}}$ or \mathbb{C}^N , then $[x]_n \in \mathbb{C}^n$ denotes the projected vector onto \mathbb{C}^n . Clearly, $[x]_{\mathbb{C}^n} = [x]_n$.

The vector space $\mathbb{C}^N = \mathbb{R}^N \oplus_{\mathbb{R}} i\mathbb{R}^N$ is isomorphic to \mathbb{R}^{2N} via the map

$$(9) \quad G(v) := \begin{bmatrix} \Re(v) \\ \Im(v) \end{bmatrix}, \quad \forall v \in \mathbb{C}^N$$

and endowed with the real inner product

$$\langle u, v \rangle := \Re(u^* v) = G(u)^\top G(v), \quad u, v \in \mathbb{C}^N.$$

With a slight abuse of notation, we will use $G(u)$ to denote the conversion of a complex-valued vector u in $\mathbb{C}^n, \mathbb{C}^{\tilde{n}}$ or \mathbb{C}^N to its real-valued version.

Phase factor: Let $y \odot y'$ and y/y' be the component-wise multiplication and division between two vectors y, y' , respectively. For any $y \in \mathbb{C}^N$ define the phase vector $\omega \in \mathbb{C}^N$ with $\omega(j) = y(j)/|y(j)|$ where $|y(j)| \neq 0$. When $|y(j)| = 0$ the phase can be assigned arbitrarily and we set $\omega(j) = 1$ unless otherwise specified.

3. DOUGLAS-RACHFORD ALGORITHM

Phase retrieval can be formulated as the following feasibility problem in the Fourier domain

$$(10) \quad \text{Find } \hat{y} \in A^* \mathcal{X} \cap \mathcal{Y}, \quad \mathcal{Y} := \{y \in \mathbb{C}^N : |y| = b\}.$$

Let P_1 be the projection onto $A^* \mathcal{X}$ and P_2 the projection onto \mathcal{Y} :

$$(11) \quad P_1 y = A^*[Ay]_{\mathcal{X}}, \quad P_2 y = b \odot \frac{y}{|y|}$$

Then DR (1) becomes $y^{(k+1)} = S_f(y^{(k)})$ with

$$(12) \quad S_f(y) = y + A^* \left[A \left(2b \odot \frac{y}{|y|} - y \right) \right]_{\mathcal{X}} - b \odot \frac{y}{|y|}$$

which we call the *Fourier-domain DR* (FDR) to contrast with the following object domain version.

Let $\tilde{A}^* = [A^*, A_\perp^*] \in \mathbb{C}^{N, \tilde{n}}$ be a complex isometric extension of A^* , implying that $A_\perp A_\perp^* = I$, $A A_\perp^* = A_\perp A^* = 0$. Then the phase retrieval problem can be more generally formulated as $|\tilde{A}^* x| = b, x \in \mathcal{X}$. Consider the feasibility problem

$$(13) \quad \text{Find } \hat{x} \in \mathcal{X} \cap \tilde{\mathcal{X}}, \quad \tilde{\mathcal{X}} := \{x \in \mathbb{C}^{\tilde{n}} : |\tilde{A}^* x| = b\}.$$

Let P_1 be the projection onto \mathcal{X} , i.e. $P_1 x = [x]_{\mathcal{X}}$, and P_2 the projection onto $\tilde{\mathcal{X}}$. When $\tilde{n} = N$ (hence \tilde{A} is unitary),

$$(14) \quad P_2 x = \tilde{A} \left(b \odot \frac{\tilde{A}^* x}{|\tilde{A}^* x|} \right)$$

and (12) is equivalent to

$$(15) \quad S(x) = x + \left[\tilde{A} \left(2b \odot \frac{\tilde{A}^* x}{|\tilde{A}^* x|} \right) - x \right]_{\mathcal{X}} - \tilde{A} \left(b \odot \frac{\tilde{A}^* x}{|\tilde{A}^* x|} \right).$$

In this case, we have

$$(16) \quad \tilde{A}^* S \tilde{A} = S_f, \quad \text{for } \tilde{n} = N.$$

In the 1-pattern case with the standard oversampling $N = \tilde{n} \approx 4n$, $\tilde{A} = A$ is unitary and (15) is also known as the Hybrid-Input-Output (HIO) algorithm (with the HIO parameter set to one) [8, 30].

For $\tilde{n} < N$ (as with two oversampled patterns $N \approx 8n$ with the standard padding $\tilde{n} \approx 4n$), the precise form of P_2 is not known explicitly. For the purpose of contrasting with (12) and for lack of a better term we shall call (15) (with $\tilde{n} \leq N$) the generalized Object-domain Douglas-Rachford algorithm (ODR for short). The ODR family is an interpolation between the HIO and FDR.

While ODR depends explicitly on \tilde{n} , FDR is independent of \tilde{n} in the sense that

$$(17) \quad S_f(y) = y + \tilde{A}^* \left[\tilde{A} \left(2b \odot \frac{y}{|y|} - y \right) \right]_{\mathcal{X}} - b \odot \frac{y}{|y|}$$

since $[\tilde{A}y]_{\mathcal{X}} = [Ay]_{\mathcal{X}} \in \mathbb{C}^n$ and $\tilde{A}^*[\tilde{A}y]_{\mathcal{X}} = A^*[Ay]_{\mathcal{X}}$.

4. LOCAL CONVERGENCE

For simplicity, we shall analyze FDR (12) *without* the sector condition:

$$(18) \quad S_f(y) := y + A^* A \left(2b \odot \frac{y}{|y|} - y \right) - b \odot \frac{y}{|y|}$$

whereas ODR (15) becomes

$$(19) \quad S(x) = x + \left[\tilde{A} \left(2b \odot \frac{\tilde{A}^* x}{|\tilde{A}^* x|} \right) - x \right]_n - \tilde{A} \left(b \odot \frac{\tilde{A}^* x}{|\tilde{A}^* x|} \right).$$

However, we make no assumption about the number of diffraction patterns which can well be one.

The main result is local, geometric convergence of the FDR algorithm.

Theorem 4.1. *Let $x_0 \in \mathbb{C}^n$ and A^* any isometric $N \times n$ matrix. Suppose $N \geq 2n$ and*

$$(20) \quad \max_{\substack{u \in \mathbb{C}^n \\ iu \perp x_0}} \|u\|^{-1} \|\Im(B^* u)\| < 1, \quad B := A \operatorname{diag} \left\{ \frac{A^* x_0}{|A^* x_0|} \right\}.$$

Let $y^{(k)}$ be an FDR sequence and $x^{(k)} := Ay^{(k)}$, $k = 1, 2, 3, \dots$. If $x^{(1)}$ is sufficient close to x_0 , then for some constant $\gamma < 1$

$$(21) \quad \|\alpha^{(k)} x^{(k)} - x_0\| \leq \gamma^{k-1} \|x^{(1)} - x_0\|, \quad \forall k,$$

where

$$(22) \quad \alpha^{(k)} := \arg \min_{\alpha} \{\|\alpha x^{(k)} - x_0\| : |\alpha| = 1, \alpha \in \mathbb{C}\}.$$

Remark 4.2. In view of (16) and Theorem 4.1, the following error bound holds for ODR with $\tilde{n} = N$

$$\|\alpha^{(k)}[x^{(k)}]_n - x_0\| \leq \gamma^{k-1} \|\alpha^{(1)}[x^{(1)}]_n - x_0\|,$$

where $x^{(k)} = \tilde{A}y^{(k)}$ and

$$(23) \quad \alpha^{(k)} = \arg \min_{\alpha \in \mathbb{C}, |\alpha|=1} \|\alpha x^{(k)} - x_0\|.$$

Remark 4.3. Theorem 4.1 is about the algebraic structure of FDR and does not assume oversampled diffraction patterns. For example, one oversampled diffraction pattern ($N \approx 4n$) or two unoversampled diffraction patterns ($N = 2n$) are sufficient.

However, as shown in Theorem 5.3, the proof of (20) requires one (and only one) oversampled coded diffraction pattern.

Remark 4.4. When the propagation matrix A^* is not isometric, we apply QR-decomposition to obtain $A^* = QR$, where Q is isometric, and treat Q as the new propagation matrix and Rx_0 as the unknown.

To this end, we derive and analyze the local approximation of FDR as follows.

4.1. Local analysis. First note that

$$(24) \quad \langle A(\alpha^{(k)}y^{(k)} - y_0), x_0 \rangle = \langle \alpha^{(k)}y^{(k)} - y_0, y_0 \rangle = \langle v^{(k)}, |y_0| \rangle$$

with

$$v^{(k)} = \Omega_0^*(\alpha^{(k)}y^{(k)} - y_0), \quad \Omega_0 = \text{diag}(\omega_0), \quad \omega_0 = \frac{y_0}{|y_0|}.$$

This motivates the following analysis of the Jacobian operator J_f .

Proposition 4.5. Let $y \in \mathbb{C}^N$, $\omega = y/|y|$ and $\Omega = \text{diag}(\omega)$.

Then

$$(25) \quad S_f(y + \epsilon\eta) - S_f(y) = \epsilon\Omega J_f v + o(\epsilon)$$

where

$$(26) \quad J_f v = (I - B^*B)v + i(2B^*B - I) \text{diag} \left[\frac{b}{|y|} \right] \Im(v),$$

with

$$(27) \quad B = A\Omega, \quad v = \Omega^*\eta.$$

In particular, if $|y| = b$, then (26) becomes

$$(28) \quad J_f v = (I - B^*B)\Re(v) + iB^*B\Im(v)$$

Proof. Let

$$\omega_\epsilon = \frac{y + \epsilon\eta}{|y + \epsilon\eta|}, \quad \Omega_\epsilon = \text{diag}(\omega_\epsilon).$$

Reorganizing (18), we have

$$(29) \quad S_f(y) = y - A^*Ay + (2A^*A - I)\Omega b.$$

and hence

$$(30) \quad \begin{aligned} S_f(y + \epsilon\eta) - S_f(y) &= \epsilon(I - A^*A)\eta + (2A^*A - I)(\Omega_\epsilon - \Omega)b \\ &= \epsilon(I - \Omega B^*B\Omega^*)\eta + (2\Omega B^*B\Omega^* - I)(\Omega_\epsilon - \Omega)b \end{aligned}$$

We next give a first order approximation to $(\Omega_\epsilon - \Omega)b$ in terms of η .

Using the first order Taylor expansion we have

$$\omega_\epsilon - \omega = i\Omega \Im \left[\Omega^* (\omega_\epsilon - \omega) \right] + o(\epsilon) = i\epsilon \Omega \Im \left[\Omega^* \frac{\eta}{|y|} \right] + o(\epsilon),$$

and hence

$$(31) \quad (\Omega_\epsilon - \Omega)b = i\epsilon \Omega \operatorname{diag} \left[\frac{b}{|y|} \right] \Im(\Omega^* \eta) + o(\epsilon).$$

Finally, substituting (31) into (30) we obtain

$$S_f(y + \epsilon \eta) - S_f(y) = \epsilon(I - \Omega B^* B \Omega^*) \eta + i\epsilon(2\Omega B^* B - \Omega) \operatorname{diag}(b/|y|) \Im(\Omega^* \eta) + o(\epsilon).$$

Multiplying Ω^* on both sides and using the definition of v we complete the proof. \square

Note that J_f is a *real*, but *not complex*, linear map since $J_f(cv) \neq cJ_f v, c \in \mathbb{C}$ in general.

Define the real form of the matrix B :

$$(32) \quad \mathcal{B} := \begin{bmatrix} \Re[B] \\ \Im[B] \end{bmatrix} \in \mathbb{R}^{2n, N}.$$

Note that

$$\begin{bmatrix} \Re[B^\top] & \Im[B^\top] \\ -\Im[B^\top] & \Re[B^\top] \end{bmatrix}$$

is real isometric because B^* is complex isometric.

From (9) we have

$$(33) \quad G(B^* u) = \begin{bmatrix} \mathcal{B}^\top G(u) \\ \mathcal{B}^\top G(-iu) \end{bmatrix}, \quad u \in \mathbb{C}^n.$$

For the rest of the paper, B denotes the matrix (27) with $\Omega = \Omega_0$, i.e.

$$(34) \quad B = A\Omega_0, \quad \Omega_0 = \operatorname{diag}[\omega_0], \quad \omega_0 = \frac{y_0}{|y_0|}$$

unless otherwise specified.

4.2. Eigen structure. Let $\lambda_1 \geq \lambda_2 \geq \dots \geq \lambda_{2n} \geq \lambda_{2n+1} = \dots = \lambda_N = 0$ be the singular values of \mathcal{B} with the corresponding right singular vectors $\{\eta_k \in \mathbb{R}^N\}_{k=1}^N$ and left singular vectors $\{\xi_k \in \mathbb{R}^{2n}\}_{k=1}^{2n}$. By definition, for $k = 1, \dots, 2n$,

$$(35) \quad B\eta_k = \lambda_k G^{-1}(\xi_k),$$

$$(36) \quad \Re[B^* G^{-1}(\xi_k)] = \lambda_k \eta_k.$$

Proposition 4.6. *We have $\xi_1 = G(x_0)$, $\xi_{2n} = G(-ix_0)$, $\lambda_1 = 1$, $\lambda_{2n} = 0$ as well as $\eta_1 = |y_0|$.*

Proof. Since

$$B^* x_0 = \Omega_0^* A^* x_0 = |y_0|$$

we have by (33)

$$(37) \quad \Re[B^* x_0] = \mathcal{B}^\top \xi_1 = |y_0|, \quad \Im[B^* x_0] = \mathcal{B}^\top \xi_{2n} = 0$$

and hence the results. \square

Corollary 4.7.

$$(38) \quad \lambda_2 = \max_{\substack{u \in \mathbb{C}^n \\ iu \perp x_0}} \|u\|^{-1} \|\Im[B^*u]\| = \max_{\substack{u \in \mathbb{R}^{2n} \\ u \perp \xi_1}} \|u\|^{-1} \|\mathcal{B}^\top u\|$$

Proof. By (33),

$$\Im[B^*u] = \mathcal{B}^\top G(-iu).$$

The orthogonality condition $iu \perp x_0$ is equivalent to

$$G(x_0) \perp G(-iu).$$

Hence, by Proposition 4.6 ξ_2 is the maximizer of the right hand side of (38), yielding the desired value λ_2 . □

Proposition 4.8. For $k = 1, \dots, n$,

$$(39) \quad \lambda_k^2 + \lambda_{2n+1-k}^2 = 1$$

$$(40) \quad \xi_{2n+1-k} = G(-iG^{-1}(\xi_k))$$

$$(41) \quad \xi_k = G(iG^{-1}(\xi_{2n+1-k})).$$

Proof. Since B^* is an isometry, we have $\|w\| = \|B^*w\|, \forall w \in \mathbb{C}^n$. On the other hand, we have

$$\|B^*w\|^2 = \|G(B^*w)\|^2 = \|\mathcal{B}^\top G(w)\|^2 + \|\mathcal{B}^\top G(-iw)\|^2$$

and hence

$$(42) \quad \|G(w)\|^2 = \|\mathcal{B}^\top G(w)\|^2 + \|\mathcal{B}^\top G(-iw)\|^2.$$

Now we prove (39), (40) and (41) by induction.

Recall the variational characterization of the singular values/vectors

$$(43) \quad \lambda_j = \max \|\mathcal{B}^\top u\|, \quad \xi_j = \arg \max \|\mathcal{B}^\top u\|, \quad \text{s.t. } u \perp \xi_1, \dots, \xi_{j-1}, \quad \|u\| = 1$$

$$(44) \lambda_{2n+1-j} = \min \|\mathcal{B}^\top u\|, \quad \xi_{2n+1-j} = \arg \min \|\mathcal{B}^\top u\|, \quad \text{s.t. } u \perp \xi_{2n}, \dots, \xi_{2n+2-j}, \|u\| = 1.$$

By Proposition 4.6, (39), (40) and (41) hold for $k = 1$. Suppose (39), (40) and (41) hold for $k = 1, \dots, j-1$ and we now show that they also hold for $k = j$.

Hence by (42)

$$\lambda_j^2 = \max_{\|u\|=1} \|\mathcal{B}^\top u\|^2 = 1 - \min_{\|v\|=1} \|\mathcal{B}^\top v\|^2, \quad \text{s.t. } u \perp \xi_1, \dots, \xi_{j-1}, \quad v = G(-iG^{-1}(u)).$$

The condition $u \perp \xi_1, \dots, \xi_{j-1}$ implies $v \perp \xi_{2n}, \dots, \xi_{2n+2-j}$ and vice versa. By (44), we have $\lambda_j^2 = 1 - \lambda_{2n+1-j}^2$ and $G(-iG^{-1}(\xi_j))$ is the minimizer, i.e. $\xi_{2n+1-j} = G(-iG^{-1}(\xi_j))$. □

The relation (39) suggests the following parametrization of singular values of \mathcal{B} :

$$\lambda_{2n+1-k} := \cos \theta_k, \quad \lambda_k := \sin \theta_k, \quad \theta_k \in [0, 2\pi].$$

Proposition 4.9. For each $k = 1, \dots, n$,

$$(45) \quad B^* B \eta_k = \lambda_k (\lambda_k \eta_k + i \lambda_{2n+1-k} \eta_{2n+1-k}),$$

$$(46) \quad B^* B \eta_{2n+1-k} = \lambda_{2n+1-k} (\lambda_{2n+1-k} \eta_{2n+1-k} - i \lambda_k \eta_k).$$

Proof. By definition, $\mathcal{B}\eta_k = \lambda_k \xi_k$. Hence

$$B\eta_k = (\Re[B] + i\Im[B])\eta_k = \lambda_k(\xi_k^R + i\xi_k^I)$$

where

$$\xi_k = \begin{bmatrix} \xi_k^R \\ \xi_k^I \end{bmatrix}, \quad \xi_k^R, \xi_k^I \in \mathbb{R}^n.$$

On the other hand, $\mathcal{B}^\top \xi_k = \lambda_k \eta_k$ and hence

$$(47) \quad \Re[B^\top]\xi_k^R + \Im[B^\top]\xi_k^I = \lambda_k \eta_k.$$

Now we compute $B^*B\eta_k$ as follows.

$$(48) \quad \begin{aligned} B^*B\eta_k &= \lambda_k B^*(\xi_k^R + i\xi_k^I) \\ &= \lambda_k(\Re[B^\top] - i\Im[B^\top])(\xi_k^R + i\xi_k^I) \\ &= \lambda_k(\Re[B^\top]\xi_k^R + \Im[B^\top]\xi_k^I) + i\lambda_k(\Re[B^\top]\xi_k^I - \Im[B^\top]\xi_k^R) \\ &= \lambda_k^2 \eta_k + i\lambda_k(\Re[B^\top]\xi_k^I - \Im[B^\top]\xi_k^R) \end{aligned}$$

by (47).

Notice that

$$(49) \quad \begin{aligned} \Re(B^\top)\xi_k^I - \Im(B^\top)\xi_k^R &= \mathcal{B}^\top \begin{bmatrix} \Re(-iG^{-1}(\xi_k)) \\ \Im(-iG^{-1}(\xi_k)) \end{bmatrix} \\ &= \mathcal{B}^\top G(-iG^{-1}(\xi_k)) \\ &= \mathcal{B}^\top \xi_{2n+1-k} \\ &= \lambda_{2n+1-k} \eta_{2n+1-k} \end{aligned}$$

by Proposition 4.8.

Putting (48) and (49) together, we have (45). (46) follows from the similar calculation. \square

Corollary 4.10. *For $k = 1, 2, \dots, 2n$, J_f leaves invariant the subspace spanned by $\{\eta_k, i\eta_{2n+1-k}\}$ and has the matrix form*

$$(50) \quad J_f = \lambda_{2n+1-k} \begin{bmatrix} \cos \theta_k & \sin \theta_k \\ -\sin \theta_k & \cos \theta_k \end{bmatrix}, \quad \lambda_{2n+1-k} := \cos \theta_k, \quad \lambda_k := \sin \theta_k$$

in the basis of $\{\eta_k, i\eta_{2n+1-k}\}$. In particular,

$$(51) \quad J_f \eta_1 = 0, \quad J_f i\eta_1 = i\eta_1$$

$$(52) \quad J_f \eta_{2n} = \eta_{2n}, \quad J_f i\eta_{2n} = 0.$$

where $\eta_1 = |y_0|$.

Proof. By Proposition 4.9, the span of η_k and $i\eta_{2n+1-k}$ is invariant under B^*B and hence under J_f for $k = 1, \dots, 2n$. Moreover, (45) and (46) imply

$$B^*B = \begin{bmatrix} \lambda_k^2 & \lambda_k \lambda_{2n+1-k} \\ \lambda_k \lambda_{2n+1-k} & \lambda_{2n+1-k}^2 \end{bmatrix}$$

in the basis of $\eta_k, i\eta_{2n+1-k}$. Hence by the definition (28) and Proposition 4.8,

$$J_f = \lambda_{2n+1-k} \begin{bmatrix} \lambda_{2n+1-k} & \lambda_k \\ -\lambda_k & \lambda_{2n+1-k} \end{bmatrix} = \lambda_{2n+1-k} \begin{bmatrix} \cos \theta_k & \sin \theta_k \\ -\sin \theta_k & \cos \theta_k \end{bmatrix}, \quad \theta_k \in \mathbb{R}.$$

Hence $\lambda_{2n+1-k}(\lambda_{2n+1-k} \pm i\lambda_k)$ are eigenvalues of J_f .

□

In the next two propositions, we give a complete characterization of the eigenstructure of J_f .

Proposition 4.11. *If $v^* \eta_k = 0, k = 1, 2, \dots, 2n - 1$, then*

$$(53) \quad Bv = 0, \quad J_f v = \Re(v).$$

Proof. The condition $v^* \eta_k = 0$ is equivalent to $\eta_k^\top \Re(v) = \eta_k^\top \Im(v) = 0$. So we have

$$G(B\Re(v)) = \begin{bmatrix} \Re(B\Re(v)) \\ \Im(B\Re(v)) \end{bmatrix} = \begin{bmatrix} \Re(B)\Re(v) \\ \Im(B)\Re(v) \end{bmatrix} = \mathcal{B}\Re(v) = 0$$

implying $B\Re(v) = 0$. Likewise, $B\Im(v) = 0$. So, we have $Bv = 0$.

By the definition of J_f and $Bv = 0$,

$$J_f v = (I - B^* B)\Re(v) + iB^* B\Im(v) = \Re(v).$$

□

Corollary 4.12. *The fixed point set of J_f contains the subspace*

$$E_1 = \text{null}_{\mathbb{R}}(\mathcal{B}) \subset \mathbb{R}^N$$

and the null space of J_f contains the subspace

$$E_0 = iE_1.$$

Moreover, if $\lambda_2 < 1$, then

$$E_2^\perp = E_0 \oplus_{\mathbb{R}} E_1$$

where

$$E_2 = \text{span}_{\mathbb{R}}\{\eta_k, i\eta_k\}_{k=1}^{2n-1}.$$

Proof. Note that η_{2n} and $i\eta_{2n}$ are excluded from E_2 because $\eta_{2n} \in E_1, i\eta_{2n} \in E_0$. On the other hand the null vector η_1 does not belong in E_0 and the eigenvector $i\eta_1$ for eigenvalue 1 does not belong in E_1 for an obvious reason.

For any $v \in \mathbb{C}^N$, we can write $v = \Re(v) + i\Im(v)$. By Proposition 4.11, if $\Re(v), \Im(v) \in E_2^\perp$, then

$$\begin{aligned} \mathcal{B}\Re(v) &= 0, & J_f(\Re(v)) &= \Re(v) \\ \mathcal{B}\Im(v) &= 0, & J_f(\Im(v)) &= 0. \end{aligned}$$

In other words, $\Re(v) \in E_1$ and $\Im(v) \in E_0$.

On the other hand, if $\lambda_2 < 1$, then $\lambda_{2n-1} > 0$ and E_2 has no nontrivial intersection with either E_0 or E_1 . Hence, $E_2^\perp = E_0 \oplus_{\mathbb{R}} E_1$.

□

4.3. Proof of Theorem 4.1. With $v^{(k)} = \Omega_0^*(\alpha^{(k)}y^{(k)} - y_0)$, we can express FDR as

$$(54) \quad v^{(k+1)} = J_f v^{(k)} + o(\|v^{(k)}\|).$$

by Proposition 4.5. Moreover,

$$\begin{aligned} (55) \quad BJ_f v &= (I - BB^*)B\Re(v) + iBB^*B\Im(v) \\ &= iB\Im(v), \quad \forall v \in \mathbb{C}^N, \end{aligned}$$

by (28) and the isometry property $BB^* = I$.

At the optimal phase $\alpha^{(k)}$ adjustment for $y^{(k)}$, we have

$$\Im(y_0^* \alpha^{(k)} y^{(k)}) = 0$$

and hence

$$(56) \quad \langle v^{(k)}, i|y_0| \rangle = \langle \alpha^{(k)} y^{(k)} - y_0, iy_0 \rangle = \langle \alpha^{(k)} y^{(k)}, iy_0 \rangle = \Re((\alpha^{(k)} y^{(k)})^* iy_0) = 0$$

which implies that $\Im(v^{(k)})$ is orthogonal to the leading right singular vector $\eta_1 = |y_0|$ of \mathcal{B} :

$$(57) \quad \eta_1^T \Im(v^{(k)}) = 0$$

cf. Proposition 4.6.

By (55) and (57),

$$\|B J_{\mathbf{f}} v^{(k)}\| = \|\mathcal{B} \Im(v^{(k)})\| = \|\mathcal{B} \Im(v^{(k)})\| \leq \lambda_2 \|\Im(v^{(k)})\|.$$

By induction for $k = 1, 2, \dots$

$$(58) \quad \|A(\alpha^{(k+1)} y^{(k+1)} - y_0)\| = \|B v^{(k+1)}\| \leq \gamma^k \|v^{(1)}\|,$$

for some $\gamma \in [\lambda_2, 1)$, if $\|v^{(1)}\|$ is sufficiently small.

Therefore for $x^{(k)} = A y^{(k)}$,

$$(59) \quad \alpha^{(k)} x^{(k)} - x_0 = B(\Omega_0^* \alpha^{(k)} y^{(k)} - \Omega_0^* y_0) = B v^{(k)}, \quad k = 1, 2, \dots$$

which tends to zero geometrically with a rate at most $\gamma < 1$.

5. SPECTRAL GAP

In this section, we prove the spectral gap condition (20) with at least *one oversampled coded* diffraction pattern. This is the immediate consequence of the following two results.

Proposition 5.1. *Let A^* be isometric and $B = A\Omega_0$. Then $\|\Im(B^*x)\| = 1$ holds for some unit vector x if and only if*

$$(60) \quad \Re(a_j^* x) \Re(a_j^* x_0) + \Im(a_j^* x) \Im(a_j^* x_0) = 0, \quad \forall j = 1, \dots, N,$$

where a_j are the columns of A , or equivalently

$$(61) \quad \frac{A^* x}{|A^* x|} = \sigma \odot \omega_0$$

where the components of σ are either 1 or -1, i.e.

$$\sigma(j) \in \{1, -1\}, \quad \forall j = 1, \dots, N.$$

Proof. We have

$$(62) \quad \begin{aligned} \Im(B^* x) &= \Im\left(\frac{\overline{A^* x_0}}{|A^* x_0|} \odot A^* x\right) \\ &= \sum_{j=1}^N \frac{\Re(a_j^* x_0) \Im(a_j^* x) - \Im(a_j^* x_0) \Re(a_j^* x)}{(\Re^2(a_j^* x_0) + \Im^2(a_j^* x_0))^{1/2}} \end{aligned}$$

and hence

$$\|\Im(B^*x)\|^2 \leq \sum_{j=1}^N \Re^2(a_j^*x) + \Im^2(a_j^*x) = \sum_{j=1}^N |a_j^*x|^2 = \|A^*x\|^2 = \|x\|^2$$

by the Cauchy-Schwartz inequality and isometry.

In view of (62), the inequality becomes an equality if and only if (60) or (61) holds. \square

Proposition 5.2. (*Uniqueness of Fourier magnitude retrieval*) Let x_0 be a given rank ≥ 2 object and μ be continuously and independently distributed on the unit circle. Let

$$B := A \operatorname{diag} \{\omega_0\}, \quad \omega_0 := \frac{A^*x_0}{|A^*x_0|}$$

where A^* is the given by (2). If

$$(63) \quad \angle A^*\hat{x} = \pm \angle A^*x_0$$

(after proper adjustment of the angles wherever the coded diffraction patterns vanish) where the \pm sign may be pixel-dependent, then almost surely $\hat{x} = cx_0$ for some constant $c \in \mathbb{R}$.

The proof of Proposition 5.2 is given in Appendix A.

Now we can prove the spectral gap theorem needed for geometric convergence of FDR.

Theorem 5.3. Let Φ be the oversampled discrete Fourier transform. Let x_0 be a rank ≥ 2 object and at least one of $\mu_j, j = 1, \dots, \ell \geq 2$, be independently and continuously distributed on the unit circle. Let

$$(64) \quad A^* = c \begin{bmatrix} \Phi \operatorname{diag} \{\mu_1\} \\ \dots \\ \Phi \operatorname{diag} \{\mu_\ell\} \end{bmatrix}$$

be isometric. Let

$$B := A \operatorname{diag} \{\omega_0\}, \quad \omega_0 := \frac{A^*x_0}{|A^*x_0|}.$$

Then with probability one

$$(65) \quad \|\Im(B^*u)\| = 1, \quad \|u\| = 1 \quad \text{iff} \quad u = \pm ix_0 / \|x_0\|$$

and hence

$$(66) \quad \lambda_2 = \max_{\substack{u \in \mathbb{C}^n \\ u \perp ix_0}} \|u\|^{-1} \|\Im(B^*u)\| < 1.$$

Proof. Note that the proof of Proposition 5.1 depends only on the fact that A^* is isometric and hence holds for at least one coded diffraction pattern, oversampled or not.

Also, the uniqueness theorem, Proposition 5.2, clearly holds as long as there is at least one oversampled coded diffraction pattern.

Now Proposition 5.1 says that (65) holds if (63) has a unique solution up to a real constant and Proposition 5.2 says that (63) indeed has a unique solution up to a real constant. The proof is complete. \square

We have the following corollary from Theorems 4.1 and 5.3.

Corollary 5.4. Let the assumptions of Theorem 5.3 be satisfied. Then the local, geometric convergence (21)-(22) holds for phase retrieval with (64) as the propagation matrix.

6. UNIQUENESS OF FIXED POINT

Let y_∞ be a fixed point of FDR (12), i.e.

$$S_f(y_\infty) = y_\infty, \quad x_\infty = Ay_\infty.$$

Let $\omega_\infty = y_\infty/|y_\infty|$ be the phase factor of the fixed point. Let

$$(67) \quad \hat{x} = [A(2b \odot \omega_\infty - y_\infty)]_{\mathcal{X}} = [2A(b \odot \omega_\infty) - x_\infty]_{\mathcal{X}},$$

where \mathcal{X} represents the sector condition in the 1-pattern case and $\mathcal{X} = \mathbb{C}^n$ in the 2-pattern case. We have from (12)

$$(68) \quad A^* \hat{x} = b \odot \omega_\infty$$

which implies

$$(69) \quad |A^* \hat{x}| = |A^* x_0|$$

$$(70) \quad \angle A^* \hat{x} = \angle y_\infty.$$

Eq. (69) is related to phase retrieval and eq. (70) magnitude retrieval problem.

Now we state the uniqueness for Fourier phase retrieval.

Proposition 6.1. *[27] (Uniqueness of Fourier phase retrieval) Let the assumptions of Theorem 5.3 hold. Let x be a solution of the phase retrieval problem (7).*

1) One-mask case $\ell = 1$. *Suppose, in addition, that $\angle x_0(j) \in [-\alpha\pi, \beta\pi], \forall j$. Then $x = e^{i\theta} x_0$ for some constant $\theta \in \mathbb{R}$ with a high probability which has a simple, lower bound*

$$(71) \quad 1 - n \left| \frac{\beta + \alpha}{2} \right|^{\llbracket S/2 \rrbracket}$$

if μ is uniformly distributed on the unit circle, where S is the sparsity of the image and $\llbracket S/2 \rrbracket$ the greatest integer less than or equal to $S/2$.

2) Two-mask case $\ell = 2$. *Suppose, in addition, that both masks are independently and continuously distributed on the unit circle and independent from each other. Then $x = e^{i\theta} x_0$ for some constant $\theta \in \mathbb{R}$ with probability one.*

The proof of Proposition 6.1 is given in [27] where more general uniqueness theorems can be found, including the $1\frac{1}{2}$ -mask case.

Theorem 6.2. *(Uniqueness of fixed point) Under the set-up of Proposition 6.1, the following statements hold for the phase retrieval problem (7).*

1) One-mask case. *With probability at least given in (71), $\hat{x} = e^{i\theta} x_0$ for some $\theta \in \mathbb{R}$.*

2) Two-mask case. *Almost surely $\hat{x} = x_\infty = e^{i\theta} x_0$ for some constant $\theta \in \mathbb{R}$.*

Remark 6.3. *With a slightly stronger assumption ([27], Theorem 6), the two-mask case in Proposition 6.1 and hence Theorem 6.2 hold for the $1\frac{1}{2}$ -mask case (4).*

Proof. By Proposition 6.1 (69) implies that $\hat{x} = e^{i\theta} x_0$ for some constant $\theta \in [0, 2\pi]$, with the only difference between case 1) and case 2) being the probability with which this statement



FIGURE 2. The original phantom without phase randomization (left), the truncated cameraman (middle) and the truncated Barbara (right).

holds. To complete the proof, we only need to consider case 2) and show $\hat{x} = x_\infty$.

By (67) $\hat{x} \in \mathcal{X}$ and by Proposition 6.1 (69) implies that with probability no less than (71) $\hat{x} = e^{i\theta}x_0$ for some constant $\theta \in \mathbb{R}$. Hence, by (70), we have

$$(72) \quad e^{i\theta}\omega_0 = \omega_\infty.$$

Substituting (72) into (67) we obtain

$$2e^{i\theta}x_0 = \hat{x} + x_\infty = e^{i\theta}x_0 + x_\infty$$

and hence $e^{i\theta}x_0 = x_\infty$. In other words,

$$x_\infty = \hat{x} = e^{i\theta}x_0.$$

□

On the other hand, for case 1), $\hat{x} = e^{i\theta}x_0$ and (70) imply $e^{i\theta}\omega_0 = \omega_\infty$ and hence

$$e^{i\theta}y_0 = e^{i\theta}b \odot \omega_0 = b \odot \omega_\infty.$$

This and (67) only lead to

$$\hat{x} = [2e^{i\theta}x_0 - x_\infty]_{\mathcal{X}} = [2\hat{x} - x_\infty]_{\mathcal{X}}.$$

7. NUMERICAL SIMULATIONS

7.1. Test images. For test images x_0 we consider the Randomly Phased Phantom (RPP) Fig. 2 (left) and the deterministic image, hereby called the Truncated Cameraman-Barbara (TCB), whose real part is the truncated cameraman, Fig. 2 (middle) and whose imaginary part is the truncated Barbara, Fig. 2 (right). The purpose of truncation is to create an unknown, loose support (dark margins) which makes the image more difficult to recover. RPP has a loose support without additional truncation. Likewise, we randomize the original phantom in order to make its reconstruction more challenging. In general, a random object

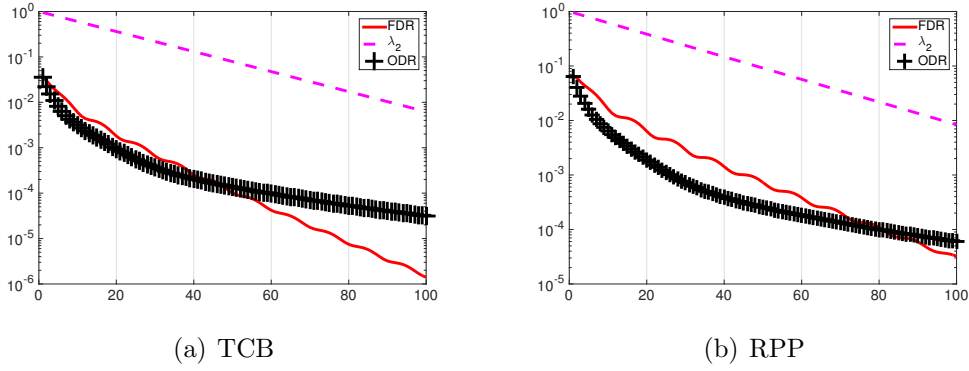


FIGURE 3. Error (on the log-scale) versus iteration for TCB (left) and RPP (right).

such as RPP is more difficult to recover than a deterministic object such as TCB (see, e.g. Fig. 5 and 7). The size n of both images is 256×256 , including the margins.

The propagation matrix is primarily based on either (2) or (4) unless specified otherwise.

7.2. Local convergence rate. First we simulate the local convergence rate of the $1\frac{1}{2}$ -mask case and compare them with λ_2 .

The initial condition $x^{(1)}$ is chosen sufficiently close to the true object x_0 , which is a unit vector. Fig. 3 shows the error $\|\alpha^{(k)}[x^{(k)}]_n - x_0\|$ on the log scale versus the iteration counter in the case of two oversampled diffraction patterns. The oscillation in the blue curve (FDR) is due to the complex eigenvalues of J_f . The magenta line shows the geometric sequence $\{\lambda_2^k\}_{k=1}^{100}$. The λ_2 value is computed via the power method, $\lambda_2 = 0.9505$ for TCB and $\lambda_2 = 0.9533$ for RPP. Note that the FDR curve (red) decays slightly faster than the λ_2 -curve (magenta), which decays still faster than the black curve (ODR with $\tilde{n} \approx 4n$).

7.3. Initialization. For *global* convergence behaviors, we test two different initializations: the Random Initialization (RI), where each pixel value is selected randomly and independently, and the Constant Initialization (CI), where each pixel value is set to unity.

The relative error of the estimate \hat{x} with the optimal phase adjustment is given by

$$(73) \quad \frac{\|e^{i\hat{\theta}}\hat{x} - x_0\|}{\|x_0\|}, \quad \hat{\theta} = \arg \min_{\theta \in \mathbb{R}} \|e^{i\theta}\hat{x} - x_0\|.$$

7.4. One-pattern case. Fig. 5 (a)-(d) shows the results of the 1-pattern case for which the sector condition is imposed (ODR is equivalent to FDR as $N = \tilde{n}$).

To test the effect of the sector constraint, the phase of RPP is uniformly distributed in two different intervals: $[0, \pi/2]$ and $[0, \pi]$. While FDR/ODR global convergence regardless the initialization is evident, the rate of convergence decreases as the sector enlarges. When the sector constraint is absent, the iteration ceases to converge in general.

7.5. $1\frac{1}{2}$ -mask case. For two- or multi-pattern case, we let the phase of RPP be uniformly distributed in $[0, 2\pi]$ (i.e. no sector constraint). Fig. 5 (e)-(h) shows the results of the $1\frac{1}{2}$ -mask case for which ODR is implemented with $\tilde{n} \approx 4n < N \approx 8n$ and hence not equivalent

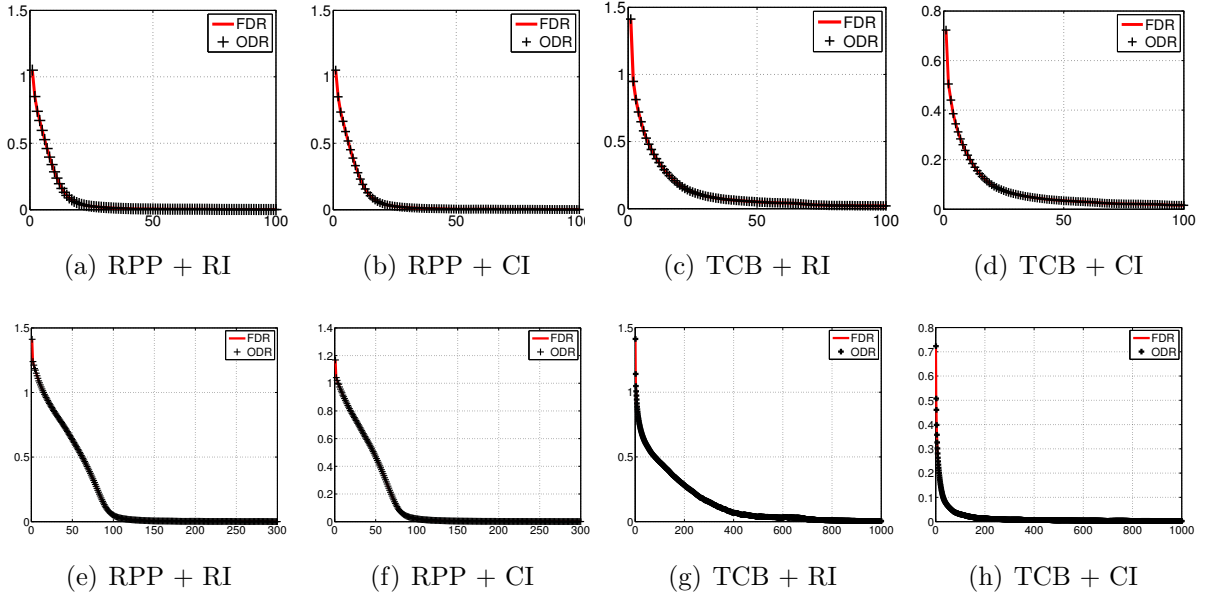


FIGURE 4. Relative error versus iteration in the 1-pattern case with two different sector constraints: $[0, \pi/2]$ for (a)-(d) and $[0, \pi]$ for (e)-(h).

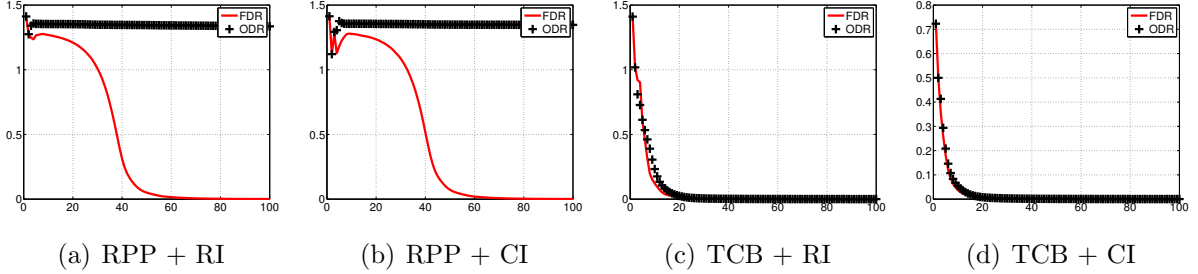


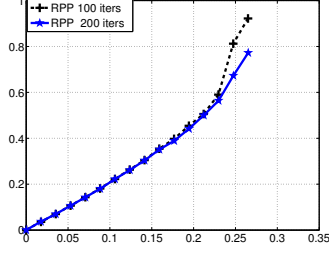
FIGURE 5. Relative error versus iteration in the $1\frac{1}{2}$ -mask case.

to FDR. We see that the performances of ODR and FDR are drastically different: While FDR converges to the true images regardless the initialization within 100 iterations, ODR does so only for the deterministic image TCB.

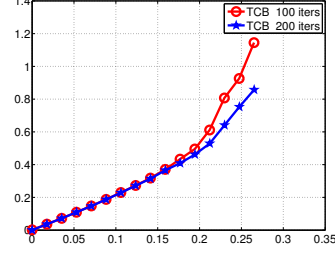
Fig. 6 shows the relative error versus noise-to-signal ratio (NSR) when noise ϵ is present in the data where

$$\text{NSR} = \frac{\|\epsilon\|}{\|A^*x_0\|}.$$

We note that for $\text{NSR} \in [0, 20\%]$ there is essentially no difference between the results with the maximum number of iterations set to 100 and 200 and this segment of error-noise curves is approximately the same straight line (slope ≈ 2.2). For a higher NSR, increasing the maximum number of iterations reduces the error so with even greater number of iterations the straight line segment can be extended to NSR greater than 20%.

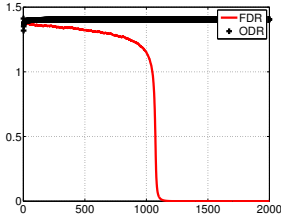


(a) RPP

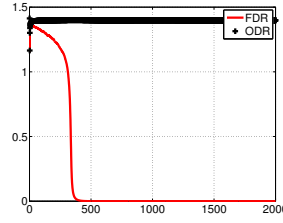


(b) TCB

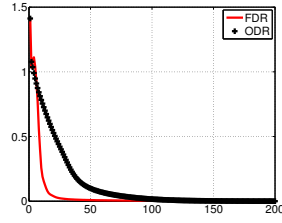
FIGURE 6. Relative error versus NSR in the $1\frac{1}{2}$ -mask case (both oversampled) with the maximum number of iteration set to 100 or 200.



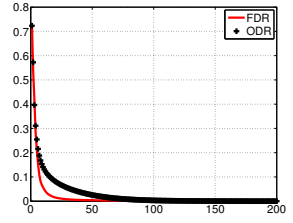
(a) RPP + RI



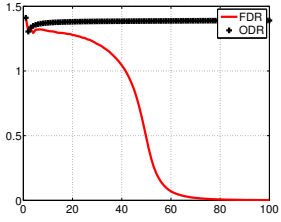
(b) RPP + CI



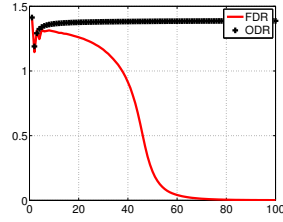
(c) TCB + RI



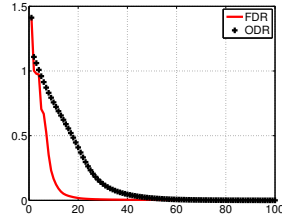
(d) TCB + CI



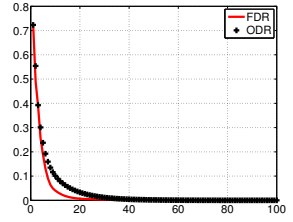
(e) RPP + RI



(f) RPP + CI



(g) TCB + RI



(h) TCB + CI

FIGURE 7. Relative error versus iteration with 3 patterns (a)-(d) and 4 patterns (e)-(h) (without oversampling in each pattern).

7.6. Multi-mask case. To test how DR performs in the setting of multiple patterns without oversampling [14, 15] we simulate the 3-pattern and 4-pattern cases with the propagation matrices

$$(74) \quad A^* = c \begin{bmatrix} \Phi \text{diag}\{\mu_1\} \\ \vdots \\ \Phi \text{diag}\{\mu_{\ell-1}\} \\ \Phi \end{bmatrix}, \quad \ell = 3, 4,$$

where Φ is the standard (unoversampled) discrete Fourier transform.

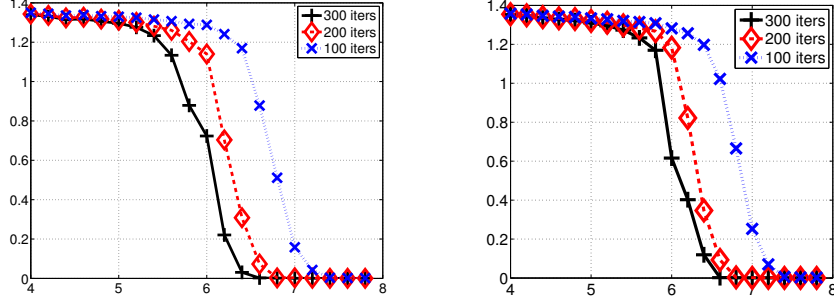


FIGURE 8. Relative error for RPP (left) and TCB (right) with various ratios \tilde{n}/n .

Figure 7 shows the result with three patterns (a)-(d) and four patterns (e)-(h), both without oversampling, i.e. $N = 3|\mathcal{M}|$ and $N = 4|\mathcal{M}|$, respectively. Note that the number of data with four patterns is half of that with 2 oversampled patterns and yet the performance of the former is almost as good as that of the latter.

Going from three patterns (Fig. 7 (a)-(b)) to four patterns (Fig. 7 (e)-(f)) reduces the number of iterations by almost an order of magnitude when RPP is the unknown image. The case with TCB has less room for improvement.

7.7. Padding ratio. Finally we test the effect of the padding ratio \tilde{n}/n on the performance of ODR. For each $\tilde{n}/n \in [4, 8]$, we conduct 50 trials with independent, random initializations and average the relative errors. Recall that $\tilde{n}/n = 4$ is the standard padding rate and at $\tilde{n}/n = 8$ ODR is equivalent to FDR.

Fig. 8 shows the averaged relative error versus the ratio \tilde{n}/n , demonstrating an effect of phase transition which depends on the number of iterations. As the number of iterations increases, the threshold ratio decreases. The phase transition accounts for the sharp transition from stagnation at the standard ratio $\tilde{n}/n = 4$ to the rapid convergence at $\tilde{n}/n = 8$ (i.e. FDR) seen in Fig. 5 (a)-(b) and Fig. 7 (a)-(b), (e)-(f).

APPENDIX A. PROOF OF PROPOSITION 5.2

In order to prove the uniqueness theorem for Fourier magnitude retrieval, we need to take up the more elaborate notation in Section 1.1.

Let

$$F(\mathbf{z}) = \sum_{\mathbf{n}} f(\mathbf{n}) \mathbf{z}^{-\mathbf{n}}$$

be the z -transform of f . According to the fundamental theorem of algebra, $F(\mathbf{z})$ can be written uniquely as

$$(75) \quad F(\mathbf{z}) = \alpha \mathbf{z}^{-\mathbf{n}_0} \prod_{k=1}^p F_k(\mathbf{z}),$$

where \mathbf{n}_0 is a vector of nonnegative integers, α is a complex coefficient, and $F_k(\mathbf{z})$ are nontrivial irreducible polynomials in \mathbf{z}^{-1} .

Define the shift

$$f_{\mathbf{m}+}(\cdot) = f(\mathbf{m} + \cdot), \quad f_{\mathbf{m}-}(\cdot) = f(\mathbf{m} - \cdot).$$

Definition 1 (Conjugate Symmetry). *A polynomial $X(\mathbf{z})$ in \mathbf{z}^{-1} is said to be conjugate symmetric if, for some vector \mathbf{k} of positive integers and some $\theta \in [0, 2\pi)$,*

$$X(\mathbf{z}) = e^{i\theta} \mathbf{z}^{-\mathbf{k}} \overline{X(\bar{\mathbf{z}}^{-1})}.$$

In other words, the ratio between $X(\mathbf{z})$ and its conjugate inversion is a monomial in \mathbf{z}^{-1} times a complex number of unit modulus.

A conjugate symmetric polynomial may be reducible, irreducible, trivial, or nontrivial. Any monomial $\mathbf{z}^{-\mathbf{k}}$ is conjugate symmetric.

Proposition A.1. *Let f be a finite array whose z -transform has no conjugate symmetric factors. If the z -transform G of another array g satisfies $\angle F(e^{2\pi i \mathbf{w}}) - \angle G(e^{2\pi i \mathbf{w}}) \in \{0, \pi\}$, $\forall \mathbf{w} \in \mathcal{L}$ then $g = cf$ for some constant $c \in \mathbb{R}$.*

The real-valued version of the above proposition is given in [36]. For the reader's convenience, we provide the proof for the complex setting.

Proof. Consider the array h defined by

$$h = f \star \overline{g(\cdot)}$$

whose z -transform is

$$H(\mathbf{z}) = F(\mathbf{z}) \overline{G(\bar{\mathbf{z}}^{-1})}.$$

Note that h is defined on $\widetilde{\mathcal{M}}$, instead of \mathcal{M} , so $H(\mathbf{z})$ is completely determined by sampling H on \mathcal{L} .

Since

$$\angle H(e^{2\pi i \mathbf{w}}) = \angle F(e^{2\pi i \mathbf{w}}) - \angle G(e^{2\pi i \mathbf{w}})$$

it follows $H(e^{2\pi i \mathbf{w}})$ is real-valued. By analytic continuation, we have

$$H(\mathbf{z}) = \overline{H(\bar{\mathbf{z}}^{-1})}$$

and

$$(76) \quad F(\mathbf{z}) \overline{G(\bar{\mathbf{z}}^{-1})} = \overline{F(\bar{\mathbf{z}}^{-1})} G(\mathbf{z}).$$

Multiplying both sides of (76) by $\mathbf{z}^{-\mathbf{M}}$ results in the following polynomial equation in \mathbf{z}^{-1} :

$$(77) \quad F(\mathbf{z}) \overline{G(\bar{\mathbf{z}}^{-1})} \mathbf{z}^{-\mathbf{M}} = \mathbf{z}^{-\mathbf{M}} \overline{F(\bar{\mathbf{z}}^{-1})} G(\mathbf{z}).$$

We observe $\mathbf{n}_0 = 0$ in view of (75) and the assumption that $F(\mathbf{z})$ has no conjugate symmetric factor. We also have

$$(78) \quad \mathbf{z}^{-\mathbf{M}} \overline{F(\bar{\mathbf{z}}^{-1})} = \tilde{\alpha} \mathbf{z}^{-\mathbf{n}_1} \prod_k \tilde{F}_k(\mathbf{z}),$$

where $\tilde{F}_k(\mathbf{z})$ are the nontrivial irreducible non-conjugate symmetric polynomials in \mathbf{z}^{-1} of the form $\tilde{F}_k(\mathbf{z}) = \mathbf{z}^{-\mathbf{M}+\mathbf{p}_k} \overline{F_k(\bar{\mathbf{z}}^{-1})}$ for some vector \mathbf{p}_k of positive integers.

Writing

$$(79) \quad G(\mathbf{z}) = \beta \mathbf{z}^{-\mathbf{m}_0} \prod_{\ell} G_{\ell}(\mathbf{z}),$$

where $G_\ell(\mathbf{z})$ are nontrivial irreducible polynomials in \mathbf{z}^{-1} , we have

$$(80) \quad \mathbf{z}^{-\mathbf{M}} \overline{G(\bar{\mathbf{z}}^{-1})} = \tilde{\beta} \mathbf{z}^{-\mathbf{m}_1} \prod_{\ell} \tilde{G}_\ell(\mathbf{z}),$$

where $\tilde{G}_\ell(\mathbf{z})$ are the nontrivial irreducible polynomials in \mathbf{z}^{-1} of the form $\tilde{G}_\ell(\mathbf{z}) = \mathbf{z}^{-\mathbf{M}+\mathbf{q}_\ell} \overline{G_\ell(\bar{\mathbf{z}}^{-1})}$ for some vector \mathbf{q}_ℓ of positive integers.

Plugging (75), (78), (79) and (80) in (77) yields

$$(81) \quad \alpha \tilde{\beta} \mathbf{z}^{-\mathbf{m}_1} \prod_k F_k(\mathbf{z}) \prod_{\ell} \tilde{G}_\ell(\mathbf{z}) = \tilde{\alpha} \beta \mathbf{z}^{-\mathbf{n}_1-\mathbf{m}_0} \prod_k \tilde{F}_k(\mathbf{z}) \prod_{\ell} G_\ell(\mathbf{z}).$$

Each nontrivial irreducible factor $F_k(\mathbf{z})$ must be equal to some $\tilde{F}_{k'}(\mathbf{z})$ or some $G_{\ell'}(\mathbf{z})$. However, if $F_k(\mathbf{z}) = \tilde{F}_k(\mathbf{z})$, then $F_k(\mathbf{z})$ is a conjugate symmetric factor. If, on the other hand, $F_k(\mathbf{z}) = \tilde{F}_{k'}(\mathbf{z})$ for some $k' \neq k$, then $F_k(\mathbf{z})F_{k'}(\mathbf{z}) = \tilde{F}_{k'}(\mathbf{z})\tilde{F}_k(\mathbf{z})$ is a conjugate symmetric factor. Both cases, however, are excluded by the assumption that the z -transform of f does not have conjugate symmetric factors.

Hence each F_k (rest. \tilde{F}_k) must be equal to some G_ℓ (rest. \tilde{G}_ℓ) and we can write

$$(82) \quad G(\mathbf{z}) = Q(\mathbf{z})F(\mathbf{z})$$

where $Q(\mathbf{z})$ is a polynomial in \mathbf{z}^{-1} , i.e.

$$Q(\mathbf{z}) = \sum_{\mathbf{n} \geq 0} c_{\mathbf{n}} \mathbf{z}^{-\mathbf{n}}.$$

By the assumption that $\angle F(e^{2\pi i \mathbf{w}}) - \angle G(e^{2\pi i \mathbf{w}}) \in \{0, \pi\}$ we have $Q(e^{2\pi i \mathbf{w}}) \in \mathbb{R}, \forall \mathbf{w} \in \mathcal{L}$, and hence $\bar{c}_{\mathbf{n}} = c_{-\mathbf{n}} = 0$ except for $\mathbf{n} = 0$ in which case $c_0 \in \mathbb{R}$. Therefore, $Q = c_0 \in \mathbb{R}$ and this is what we start out to prove. \square

Proposition A.2. [27] *Let x_0 have rank ≥ 2 . Let $\{\mu(\mathbf{n})\}$ be independent and continuous random variables on the unit circle of the complex plane. Then, the z -transform $F(\mathbf{z})$ of $f(\mathbf{n}) := \mu(\mathbf{n})x_0(\mathbf{n})$ is irreducible up to a power of \mathbf{z}^{-1} with probability one.*

For the proof of Proposition A.2 see Theorem 2 of [27].

We next show that the z -transform of $\{\mu(\mathbf{n})x_0(\mathbf{n})\}$ is almost surely irreducible up to a power \mathbf{z}^{-1} and not conjugate symmetric.

Proposition A.3. *Let $\{\mu(\mathbf{n})\}$ be independent and continuous random variables on the unit circle of the complex plane. Let $f(\mathbf{n}) := \mu(\mathbf{n})x_0(\mathbf{n})$. Then the z -transforms of both $f_{\mathbf{t}+}$ and $\overline{f_{\mathbf{t}-}}$ are almost surely not conjugate symmetric $\forall \mathbf{t}$.*

Proof. The z -transform

$$(83) \quad F_{\mathbf{t}+}(\mathbf{z}) = \sum_{\mathbf{n}} f(\mathbf{t} + \mathbf{n}) \mathbf{z}^{-\mathbf{n}}.$$

is conjugate symmetric if

$$(84) \quad F_{\mathbf{t}+}(\mathbf{z}) = e^{i\theta} \mathbf{z}^{-\mathbf{k}} \overline{F_{\mathbf{t}+}(\bar{\mathbf{z}}^{-1})}$$

for some vector \mathbf{k} of positive integers and some $\theta \in [0, 2\pi)$. Plugging (83) in (84) yields

$$\sum_{\mathbf{n}} f(\mathbf{t} + \mathbf{n}) \mathbf{z}^{-\mathbf{n}} = e^{i\theta} \mathbf{z}^{-\mathbf{k}} \sum_{\mathbf{n}'} \overline{f(\mathbf{t} + \mathbf{n}')} \mathbf{z}^{\mathbf{n}'},$$

which implies

$$(85) \quad f(\mathbf{t} + \mathbf{n}) = e^{i\theta} \overline{f(\mathbf{t} + \mathbf{k} - \mathbf{n})}, \quad \forall \mathbf{n}.$$

However, x_0 is deterministic, and $\{\mu(\mathbf{n})\}$ are independent and continuous random variables on \mathbb{S}^1 , so (85) fails with probability one for any \mathbf{k} . There are finitely many choices of \mathbf{k} , so the z -transform of $f_{\mathbf{t}+}$ is almost surely not conjugate symmetric.

Similarly, the z -transform of $\overline{f_{\mathbf{t}-}}$ is also almost surely *not* conjugate symmetric. \square

Acknowledgements. Research is supported in part by US NSF grant DMS-1413373 and Simons Foundation grant 275037.

REFERENCES

- [1] P. F. Almoró and S. G. Hanson, “Random phase plate for wavefront sensing via phase retrieval and a volume speckle field,” *Appl. Opt.* **47**, 2979-2987 (2008).
- [2] R. Balan, “Stability of phase retrievable frames”, arXiv preprint, arXiv:1308.5465, 2013.
- [3] R. Balan, B. G. Bodmann, P. G. Casazza and D. Edidin, “Painless reconstruction from magnitudes of frame coefficients,” *J Fourier Anal Appl* **15**, 488-501 (2009).
- [4] R. Balan, P. Casazza and D. Edidin, “On signal reconstruction without phase,” *Appl. Comput. Harmon. Anal.* **20**, 345-356 (2006).
- [5] R. Balan, Y. Wang, “Invertibility and robustness of phaseless reconstruction”, arXiv preprint, arXiv:1308.4718, 2013.
- [6] A. S. Bandeira, J. Cahill, D. G. Mixon, A. A. Nelson, “Saving phase: Injectivity and stability for phase retrieval,” *Appl. Comput. Harmon. Anal.* **37**, 106-125 (2014).
- [7] A. S. Bandeira, Y. Chen and D. Mixon, “Phase retrieval from power spectra of masked signals,” *Inform. Infer.* (2014) 1-20.
- [8] H.H. Bauschke, P.L. Combettes and D. R. Luke, “Phase retrieval, error reduction algorithm, and Fienup variants: a view from convex optimization,” *J. Opt. Soc. Am. A* **19**, 13341-1345 (2002).
- [9] H. H. Bauschke, P. L. Combettes, and D. R. Luke, “Finding best approximation pairs relative to two closed convex sets in Hilbert spaces,” *J. Approx. Th.* **127**, 178-192 (2004).
- [10] M. Born and E. Wolf, *Principles of Optics*, 7-th edition, Cambridge University Press, 1999.
- [11] R. Bräuer, U. Wojak, F. Wyrowski, O. Bryngdahl, “Digital diffusers for optical holography,” *Opt. Lett.* **16**, 1427-1429 (1991).
- [12] E.J. Candès, Y.C. Eldar, T. Strohmer, and V. Voroninski, “Phase retrieval via matrix completion,” *SIAM J. Imaging Sci.* **6**, 199-225 (2013).
- [13] E. J. Candès, X. Li and M. Soltanolkotabi, “Phase retrieval via Wirtinger flow: theory and algorithms,” *IEEE Trans Inform. Th.* **61**(4), 1985–2007 (2015).
- [14] E. J. Candès, X. Li and M. Soltanolkotabi. “Phase retrieval from coded diffraction patterns.” *Appl. Comput. Harmon. Anal.* **39**, 277-299 (2015).
- [15] E.J. Candès, T. Strohmer, and V. Voroninski, “Phaselift: exact and stable signal recovery from magnitude measurements via convex programming,” *Comm. Pure Appl. Math.* **66**, 1241-1274 (2012).
- [16] J. Cahill, P. Casazza, J. Peterson, L. Woodland, “Phase retrieval by projections, arXiv preprint,” arXiv:1305.6226, 2013.
- [17] Center for X-ray Optics, Lawrence Berkeley National Laboratory, <http://henke.lbl.gov>
- [18] A. Chai, M. Moscoso, G. Papanicolaou, “Array imaging using intensity-only measurements,” *Inverse Problems* **27** (1) (2011).
- [19] H.N. Chapman *et al.* “Femtosecond X-ray protein nanocrystallography”. *Nature* **470**, 73-77 (2011).
- [20] H. N. Chapman, C. Caleman and N. Timneanu, “Diffraction before destruction,” *Phil. Trans. R. Soc. B* **369** 20130313 (2014).
- [21] P. Chen, A. Fannjiang and G.-R. Liu, “Phase retrieval with coded diffraction patterns by Error Reduction algorithm,” preprint.
- [22] L. Demanet and P. Hand, “Stable optimizationless recovery from phaseless linear measurements,” *J. Fourier Anal. Appl.* **20**, 199-221 (2014).

- [23] J. Douglas and H.H. Rachford, "On the numerical solution of heat conduction problems in two and three space variables," *Trans. Am. Math. Soc.* **82**, 421-439 (1956).
- [24] J. Eckstein and D.P. Bertsekas, "On the Douglas-Rachford splitting method and the proximal point algorithm for maximal monotone operators," *Math. Program. A* **55**, 293-318 (1992).
- [25] Y.C. Eldar, S. Mendelson, "Phase retrieval: Stability and recovery guarantees," available online: arXiv:1211.0872.
- [26] C. Falldorf, M. Agour, C. v. Kopylow and R. B. Bergmann, "Phase retrieval by means of a spatial light modulator in the Fourier domain of an imaging system," *Appl. Opt.* **49**, 1826-1830 (2010).
- [27] A. Fannjiang, "Absolute uniqueness of phase retrieval with random illumination," *Inverse Problems* **28**, 075008 (2012).
- [28] A. Fannjiang and W. Liao, "Phase retrieval with random phase illumination," *J. Opt. Soc. A* **29**, 1847-1859 (2012).
- [29] A. Fannjiang and W. Liao, "Fourier phasing with phase-uncertain mask," *Inverse Problems* **29** 125001 (2013).
- [30] J. R. Fienup, "Phase retrieval algorithms: a comparison," *Appl. Opt.* **21**, 2758-2769 (1982).
- [31] J.R. Fienup, "Phase retrieval algorithms: a personal tour ", *Appl. Opt.* **52** 45-56 (2013).
- [32] R. W. Gerchberg and W. O. Saxton, "A practical algorithm for the determination of the phase from image and diffraction plane pictures," *Optik* **35**, 237-246 (1972).
- [33] D. Gross, F. Krahmer, R. Kueng, "A partial derandomization of phaselift using spherical designs", arXiv:1310.2267, 2013.
- [34] Hardy, J. W., *Adaptive Optics for Astronomical Telescopes*, New York: Oxford University Press, 1998.
- [35] H.A. Hauptman, "The phase problem of X-ray crystallography," *Rep. Prog. Phys.* **54**, 1427-1454 (1991).
- [36] M. Hayes, "The reconstruction of a multidimensional sequence from the phase or magnitude of its Fourier transform," *IEEE Trans. Acoust. Speech Signal Process* **30**, 140-154 (1982).
- [37] K. Jaganathan, S. Oymak, B. Hassibi, "On robust phase retrieval for sparse signals," in: 50th Annual Allerton Conference on Communication, Control, and Computing (Allerton), 2012, pp. 794-799.
- [38] X. Li, V. Voroninski, "Sparse signal recovery from quadratic measurements via convex programming," *SIAM J. Math. Anal.* **45** (5) (2013) 3019-3033.
- [39] P.-L. Lions and B. Mercier, "Splitting algorithms for the sum of two nonlinear operators," *SIAM J. Num. Anal.* **16**, 964-979 (1979).
- [40] A.M. Maiden, G.R. Morrison, B. Kaulich, A. Gianoncelli & J.M. Rodenburg, "Soft X-ray spectromicroscopy using ptychography with randomly phased illumination," *Nat. Commun.* **4**, 1669 (2013).
- [41] S. Marchesini, "A unified evaluation of iterative projection algorithms for phase retrieval," *Rev. Sci. Instr.* **78**, 011301 (2007).
- [42] J. Miao, P. Charalambous, J. Kirz and D. Sayre, "Extending the methodology of X-ray crystallography to allow imaging of micrometre-sized non-crystalline specimens," *Nature* **400**, 342-344 (1999).
- [43] J. Miao, J. Kirz and D. Sayre, "The oversampling phasing method," *Acta Cryst. D* **56**, 1312-1315 (2000).
- [44] J. Miao, D. Sayre and H.N. Chapman, "Phase retrieval from the magnitude of the Fourier transforms of nonperiodic objects," *J. Opt. Soc. Am. A* **15** 1662-1669 (1998).
- [45] A. Migukin, V. Katkovnik and J. Astola, "Wave field reconstruction from multiple plane intensity-only data: augmented Lagrangian algorithm," *J. Opt. Soc. Am. A* **28**, 993-1002 (2011).
- [46] Millane, R. P., Chen, J. P. L., "Aspects of direct phasing in femtosecond nanocrystallography," *Philos. Trans. R. Soc. London Ser. B* **369**, 2013.0498 (2014).
- [47] P. Netrapalli, P. Jain, S. Sanghavi, "Phase retrieval using alternating minimization," arXiv preprint, arXiv:1306.0160v2, 2015.
- [48] R. Neutze, R. Wouts, D. van der Spoel, E. Weckert, J. Hajdu, "Potential for biomolecular imaging with femtosecond x-ray pulses," *Nature* **406** 753-757 (2000).
- [49] H. Ohlsson, A.Y. Yang, R. Dong, S.S. Sastry, "Compressive phase retrieval from squared output measurements via semidefinite programming," arXiv preprint, arXiv:1111.6323, 2011.

- [50] T. Osaka, M. Yabashi, Y. Sano, K. Tono, Y. Inubushi, T. Sato, S. Matsuyama, T. Ishikawa, and K. Yamauchi, “A Bragg beam splitter for hard x-ray free-electron lasers,” *Opt. Exp.* **21**, 2823-2831 (2013).
- [51] S. Oymak, A. Jalali, M. Fazel, Y.C. Eldar, B. Hassibi, “Simultaneously structured models with application to sparse and low-rank matrices,” arXiv preprint, arXiv:1212.3753, 2012.
- [52] J. Ranieri, A. Chebira, Y.M. Lu, M. Vetterli, “Phase retrieval for sparse signals: uniqueness conditions,” arXiv preprint, arXiv:1308.3058, 2013.
- [53] M.M. Seibert *et. al* “Single mimivirus particles intercepted and imaged with an X-ray laser.” *Nature* **470**, U78-U86 (2011).
- [54] I. Waldspurger, A. d’Aspremont and S. Mallat, “Phase recovery, maxCut and complex semidefinite programming,” arXiv:1206.0102.
- [55] Z. Wen, C. Yang, X. Liu and S. Marchesini, “Alternating direction methods for classical and ptychographic phase retrieval,” *Inverse Problems* **28**, 115010 (2012).
- [56] P. Yin and J. Xin, “Phaseliftoff: an accurate and stable phase retrieval method based on difference of trace and Frobenius norms,” *Commun. Math. Sci.* **13** (2015).

APPLIED MATHEMATICS, NATIONAL CHUNG HSING UNIVERSITY, TAICHUNG 402, TAIWAN.

DEPARTMENT OF MATHEMATICS, UNIVERSITY OF CALIFORNIA, DAVIS, CALIFORNIA 95616, USA.